

Electronic supplementary information for

**Geometric and electronic properties of Si-atom-doped Al clusters:
Robustness of binary superatoms against charging**

Minoru Akutsu,^a Kiichirou Koyasu,^{a,1} Junko Atobe,^a Ken Miyajima,^{a,2} Masaaki Mitsui,^{a,3}
Hironori Tsunoyama,^a and Atsushi Nakajima^{a,b,*}

^a Department of Chemistry, Faculty of Science and Technology, Keio University
3-14-1, Hiyoshi, Kohoku-Ku, Yokohama 223-8522, Japan

^b Keio Institute of Pure and Applied Science (KiPAS), Keio University, 3-14-1 Hiyoshi, Kohoku-ku,
Yokohama 223-8522, Japan

(Received;)

Index

Full citation of Ref. 60.	S2
Figure S1. Photoionization efficiency plots for Al _n clusters (<i>n</i> = 7, 10, 11, 12, and 14–32).	S3
Figure S2. Photoionization efficiency plots for Al _n Si clusters (<i>n</i> = 7, 9, 11, and 13–31).	S4
Figure S3. Photoionization efficiency plots for Al _n Si ₂ clusters (<i>n</i> = 7 and 9–30).	S5
Figure S4. Optimized Geometries of (a) Al ₁₀ Si ^{-0/+} , (b) Al ₁₂ Si ^{-0/+} , and (c) Al ₁₁ Si ₂ ^{-0/+} with Mulliken population.	S6
Figure S5. Occupied and virtual frontier orbitals from HOMO – 9 to LUMO + 4 for Al ₁₂ Si.	S7
Figure S6. Occupied and virtual frontier orbitals from HOMO – 9 to LUMO + 4 for Al ₁₂ Si ⁻ .	S7
Figure S7. Occupied and virtual frontier orbitals from HOMO – 9 to LUMO + 3 for Al ₁₁ Si ₂ ⁺ .	S8
Figure S8. Occupied and virtual frontier orbitals from HOMO – 9 to LUMO + 3 for Al ₁₁ Si ₂ .	S8
Figure S9. Occupied and virtual frontier orbitals from HOMO – 9 to LUMO + 4 for Al ₁₁ Si ₂ ⁻ .	S9
Figure S10. Occupied and virtual frontier orbitals from HOMO – 9 to LUMO + 4 for Al ₁₂ SiF ⁻ .	S9
Figure S11. The relative reactivity for the cationic Al _n Si ₂ ⁺ clusters at <i>n</i> = 7–17 against O ₂ .	S10
Figure S12. Calculated energy diagram and orbital shapes of <i>bi</i> -icosahedral Al ₂₁ Si ₂ .	S11-12

*Corresponding address. Email address: nakajima@chem.keio.ac.jp FAX: +81-45-566-1697.

Present addresses

- 1) Department of Chemistry, School of Science, The University of Tokyo, 7-3-1 Hongo, Bunkyo-ku, Tokyo 113-0033, Japan
- 2) Department of Basic Science, School of Arts and Sciences, The University of Tokyo, Komaba, Meguro-ku, Tokyo 153-8902, Japan
- 3) Department of Chemistry, College of Science, Rikkyo University, 3-34-1, Nishiikebukuro, Toshima-ku, Tokyo 171-8501, Japan

Full citation of Ref. 60.

M. J. Frisch, G. W. Trucks, H. B. Schlegel, G. E. Scuseria, M. A. Robb, J. R. Cheeseman, G. Scalmani, V. Barone, B. Mennucci, G. A. Petersson, H. Nakatsuji, M. Caricato, X. Li, H. P. Hratchian, A. F. Izmaylov, J. Bloino, G. Zheng, J. L. Sonnenberg, M. Hada, M. Ehara, K. Toyota, R. Fukuda, J. Hasegawa, M. Ishida, T. Nakajima, Y. Honda, O. Kitao, H. Nakai, T. Vreven, J. A. Montgomery, Jr., J. E. Peralta, F. Ogliaro, M. Bearpark, J. J. Heyd, E. Brothers, K. N. Kudin, V. N. Staroverov, T. Keith, R. Kobayashi, J. Normand, K. Raghavachari, A. Rendell, J. C. Burant, S. S. Iyengar, J. Tomasi, M. Cossi, N. Rega, J. M. Millam, M. Klene, J. E. Knox, J. B. Cross, V. Bakken, C. Adamo, J. Jaramillo, R. Gomperts, R. E. Stratmann, O. Yazyev, A. J. Austin, R. Cammi, C. Pomelli, J. W. Ochterski, R. L. Martin, K. Morokuma, V. G. Zakrzewski, G. A. Voth, P. Salvador, J. J. Dannenberg, S. Dapprich, A. D. Daniels, O. Farkas, J. B. Foresman, J. V. Ortiz, J. Cioslowski and D. J. Fox, *Gaussian 09, Revision E.01*, Gaussian, Inc., Wallingford, CT, 2013.

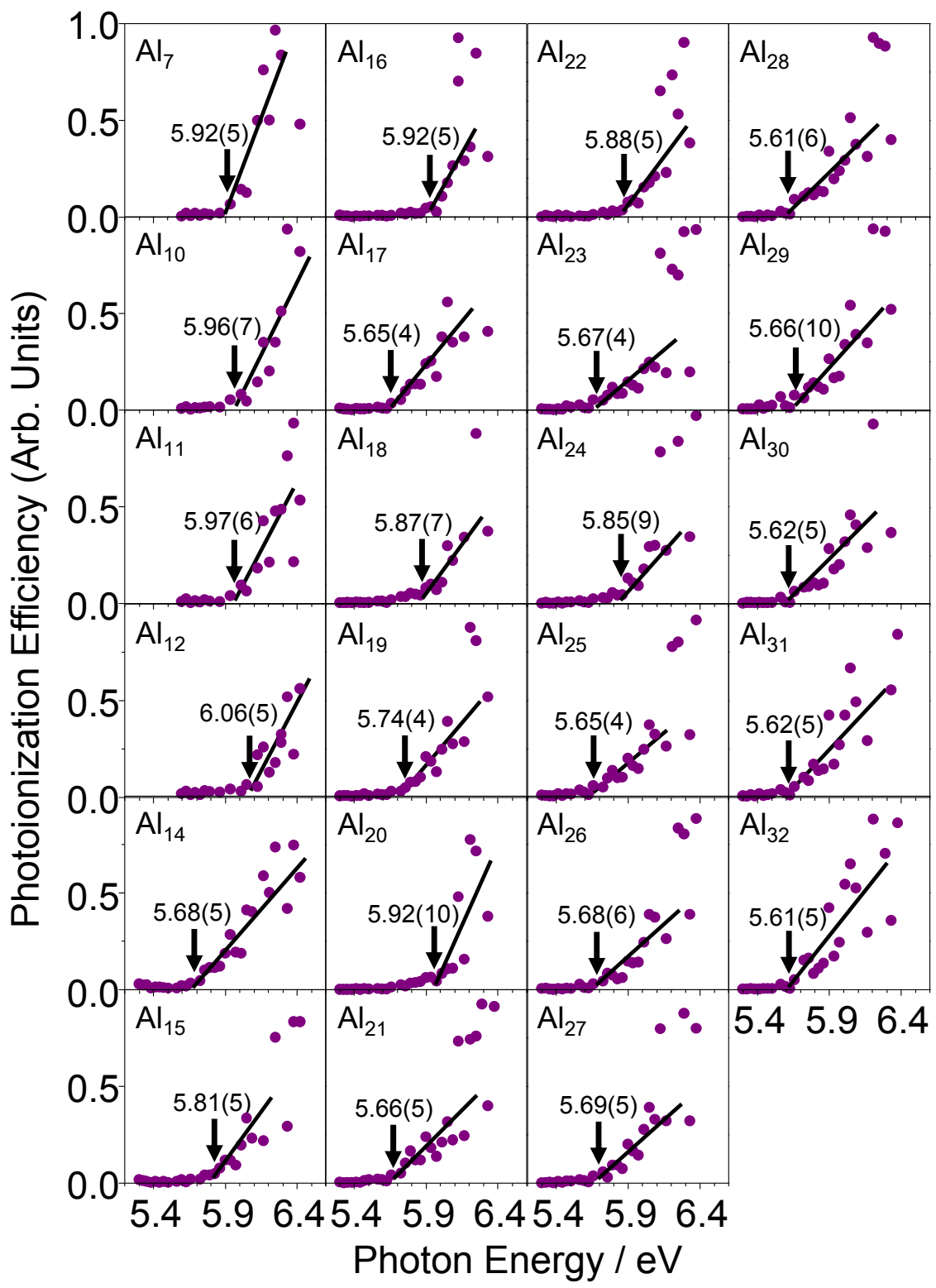


Figure S1. Photoionization efficiency plots for Al_n clusters ($n = 7, 10, 11, 12$, and 14–32) with ionization energy values, where uncertainties are given in parentheses in the last digit(s).

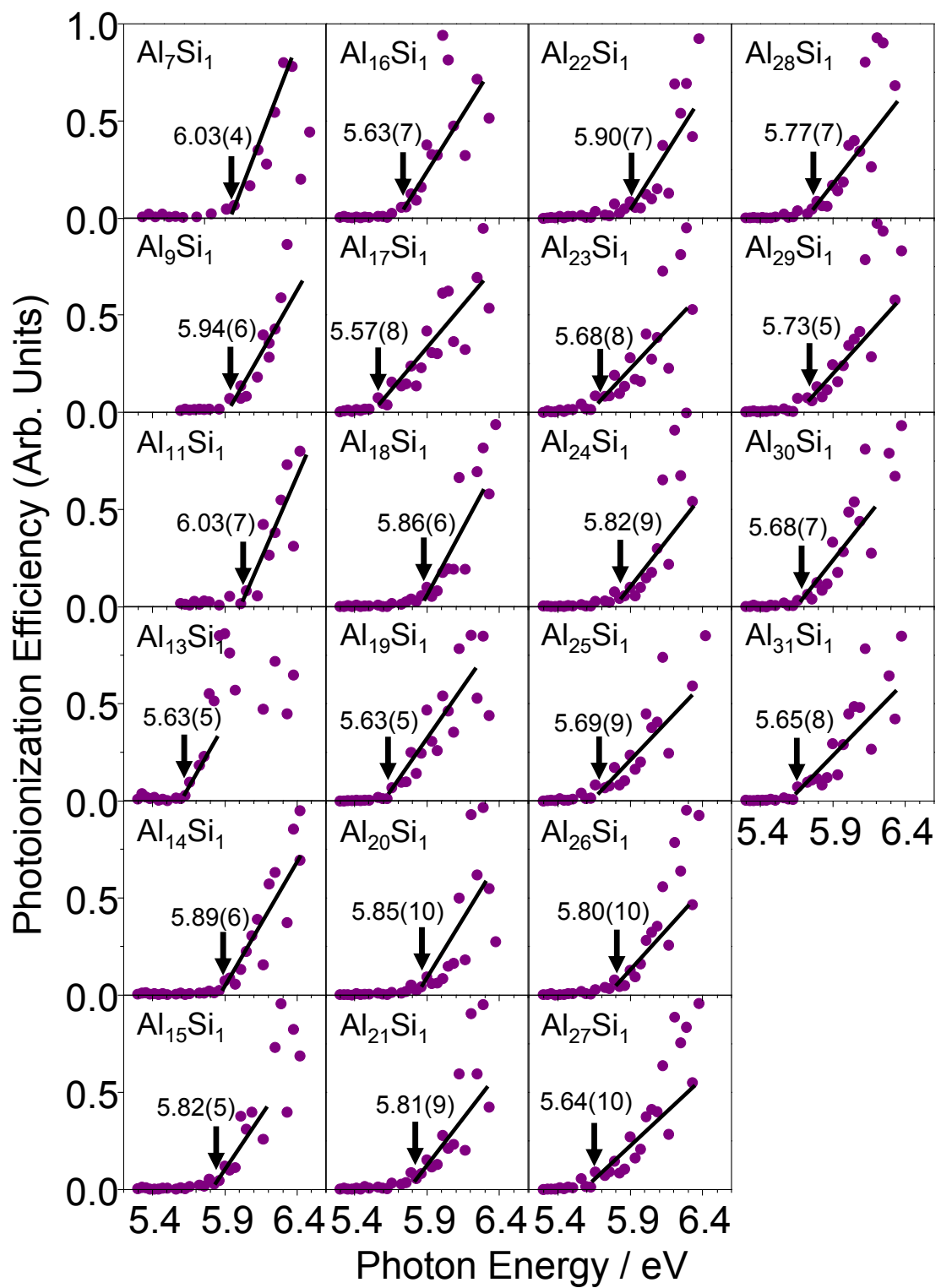


Figure S2. Photoionization efficiency plots for Al_nSi_1 clusters ($n = 7, 9, 11$, and $13-31$) with ionization energy values, where uncertainties are given in parentheses in the last digit(s).

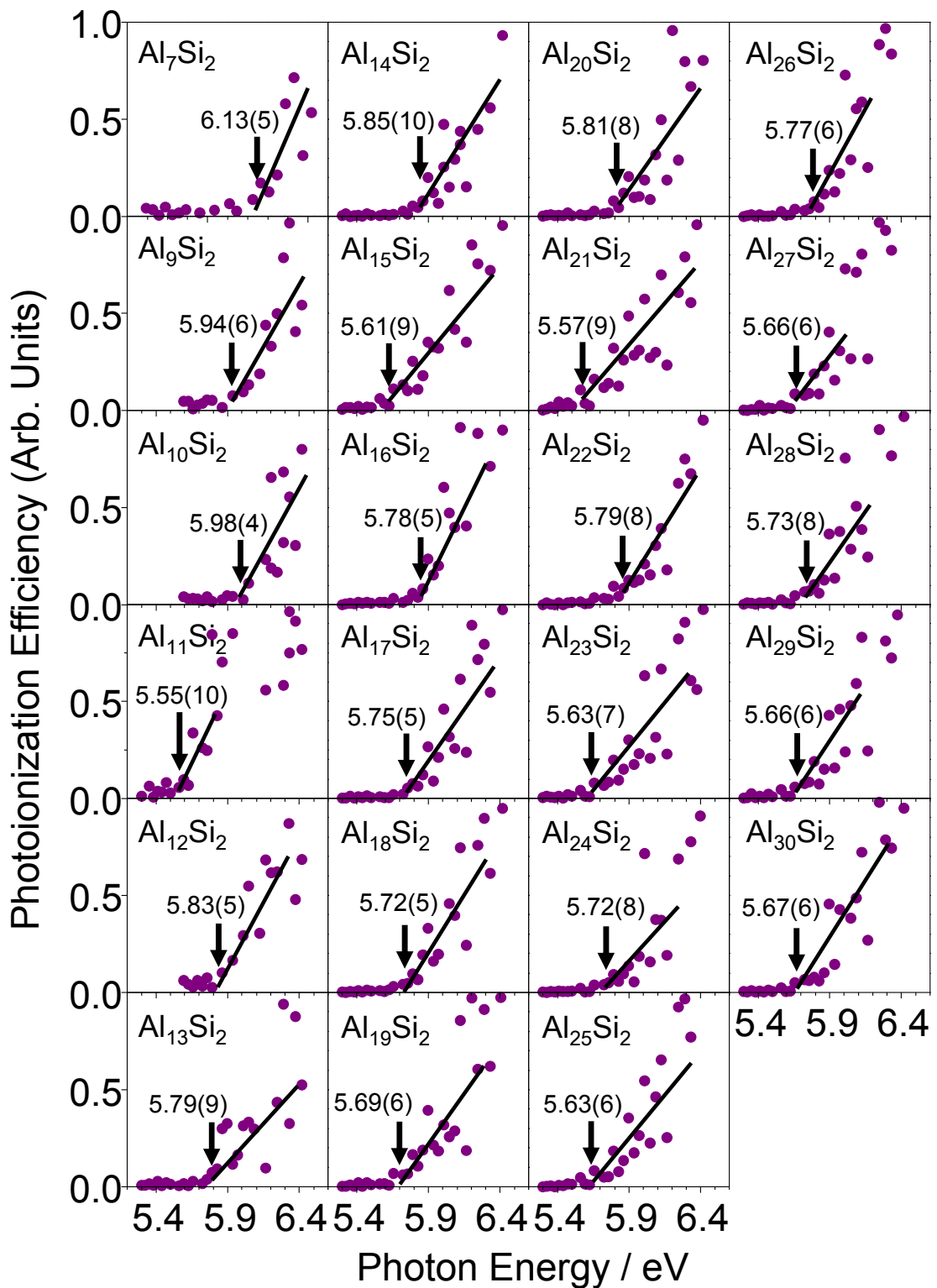


Figure S3. Photoionization efficiency plots for Al_nSi_2 clusters ($n = 7$ and 9–30) with ionization energy values, where uncertainties are given in parentheses in the last digit(s).

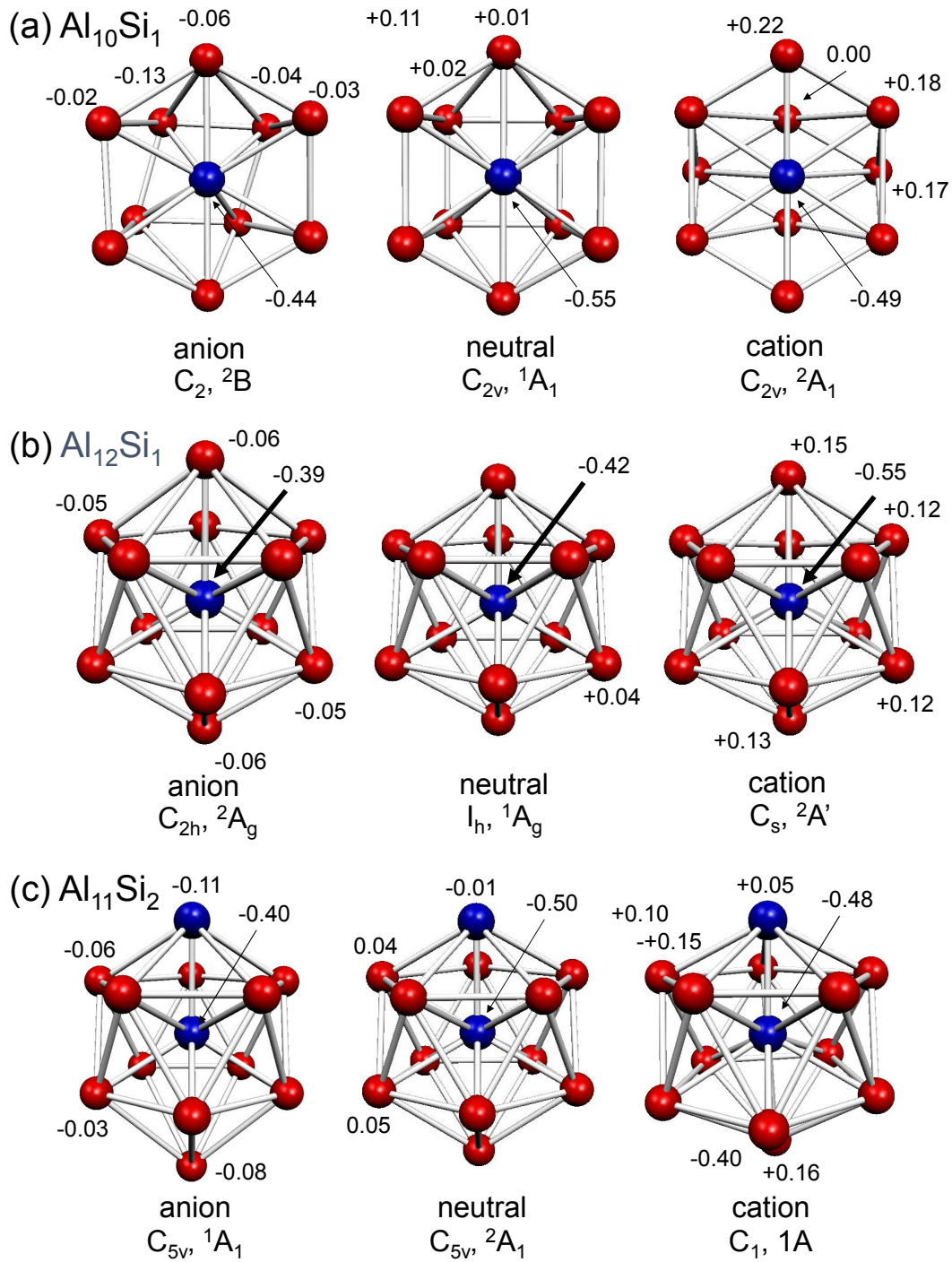


Figure S4. Optimized Geometries of (a) $\text{Al}_{10}\text{Si}^{-/0/+}$, (b) $\text{Al}_{12}\text{Si}^{-/0/+}$, and (c) $\text{Al}_{11}\text{Si}_2^{-/0/+}$ with Mulliken populations.

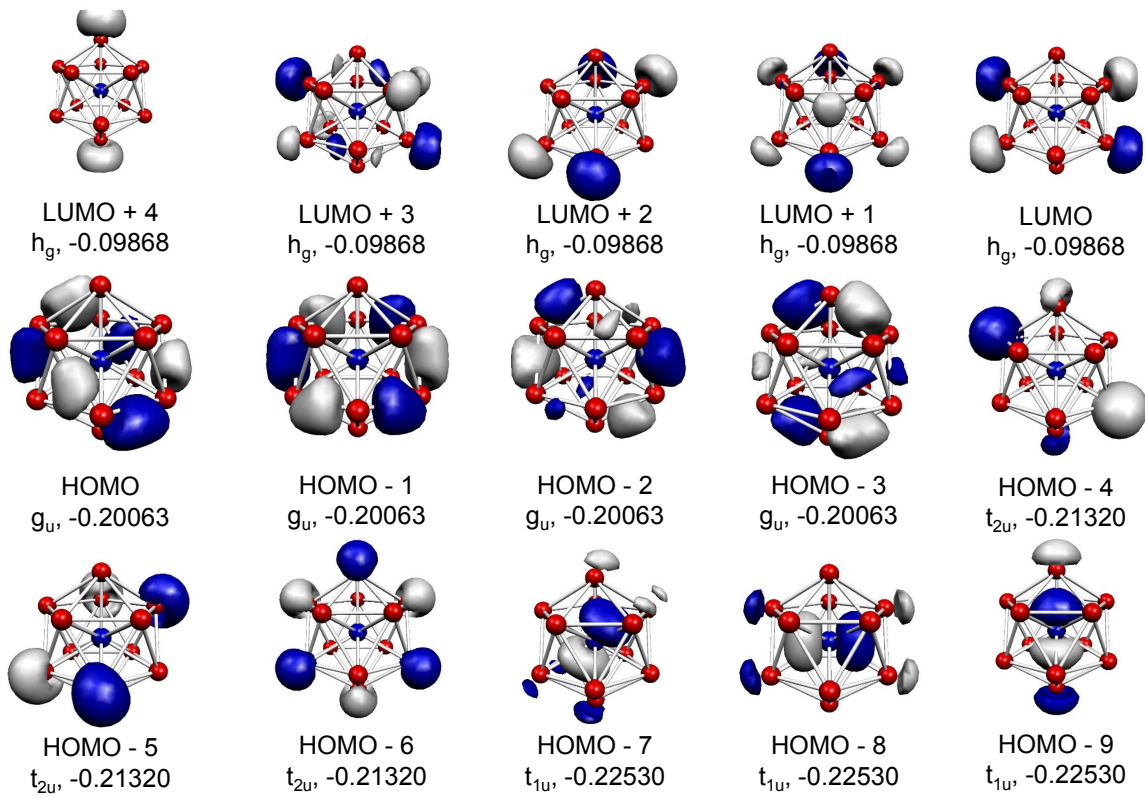


Figure S5. Occupied and virtual frontier orbitals from HOMO – 9 to LUMO + 4 for Al₁₂Si.

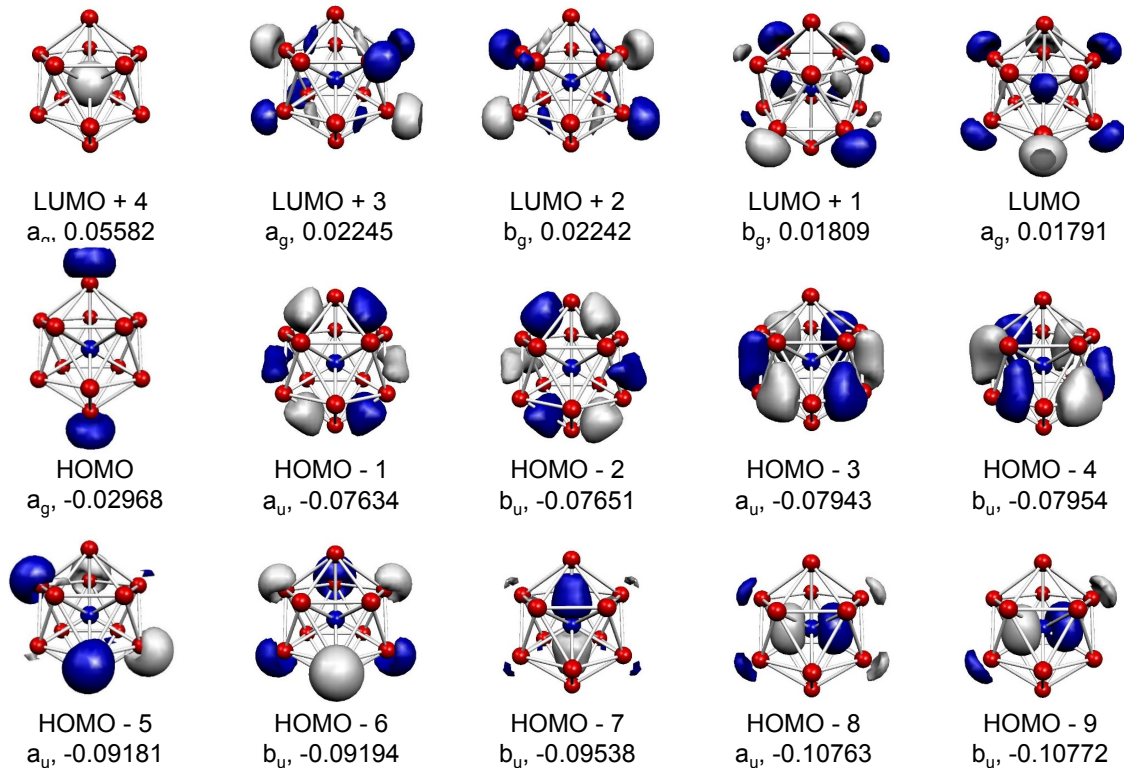


Figure S6. Occupied and virtual frontier orbitals from HOMO – 9 to LUMO + 4 for Al₁₂Si⁻.

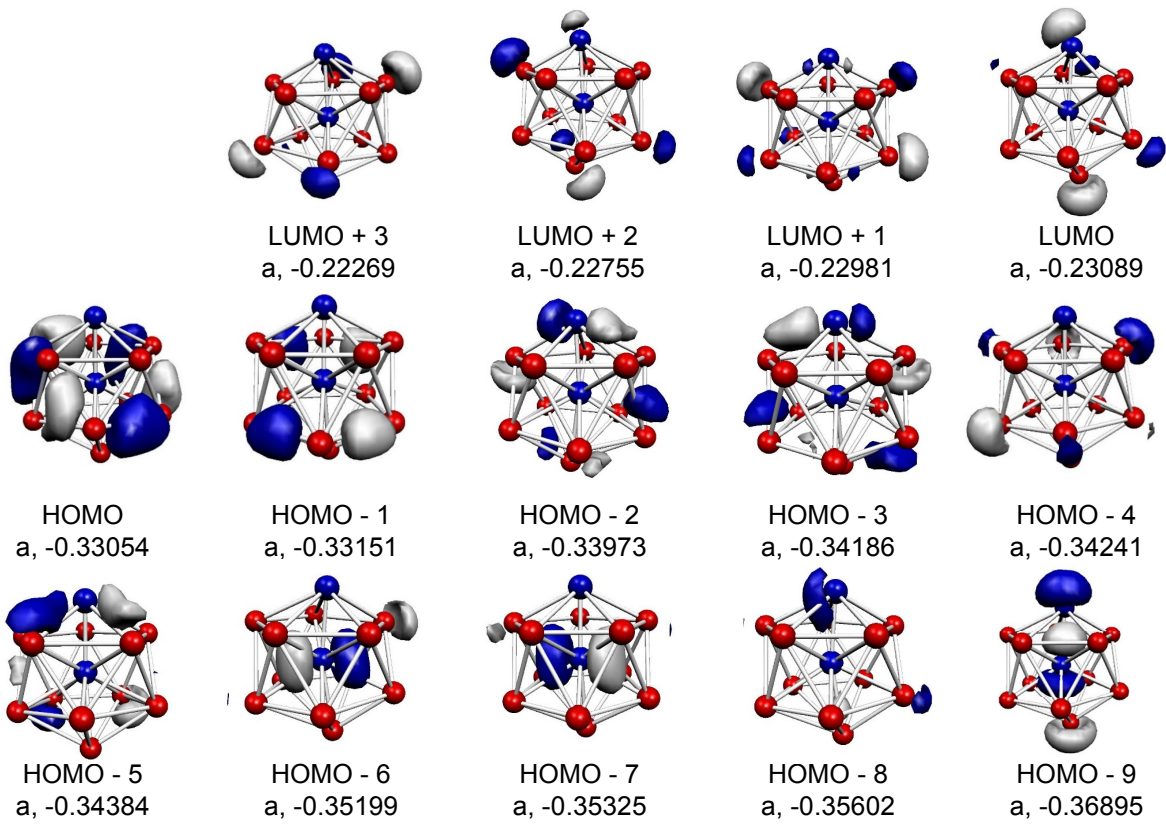


Figure S7. Occupied and virtual frontier orbitals from HOMO – 9 to LUMO + 3 for $\text{Al}_{11}\text{Si}_2^+$

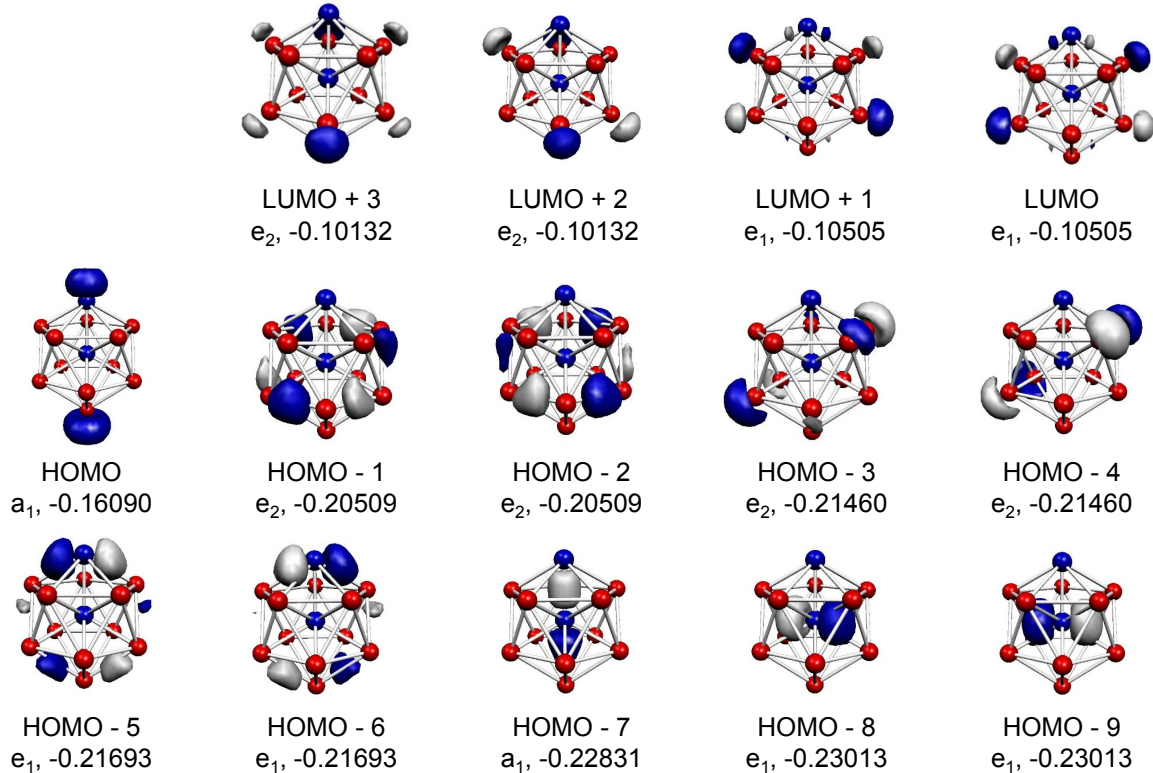


Figure S8. Occupied and virtual frontier orbitals from HOMO – 9 to LUMO + 3 for $\text{Al}_{11}\text{Si}_2$.

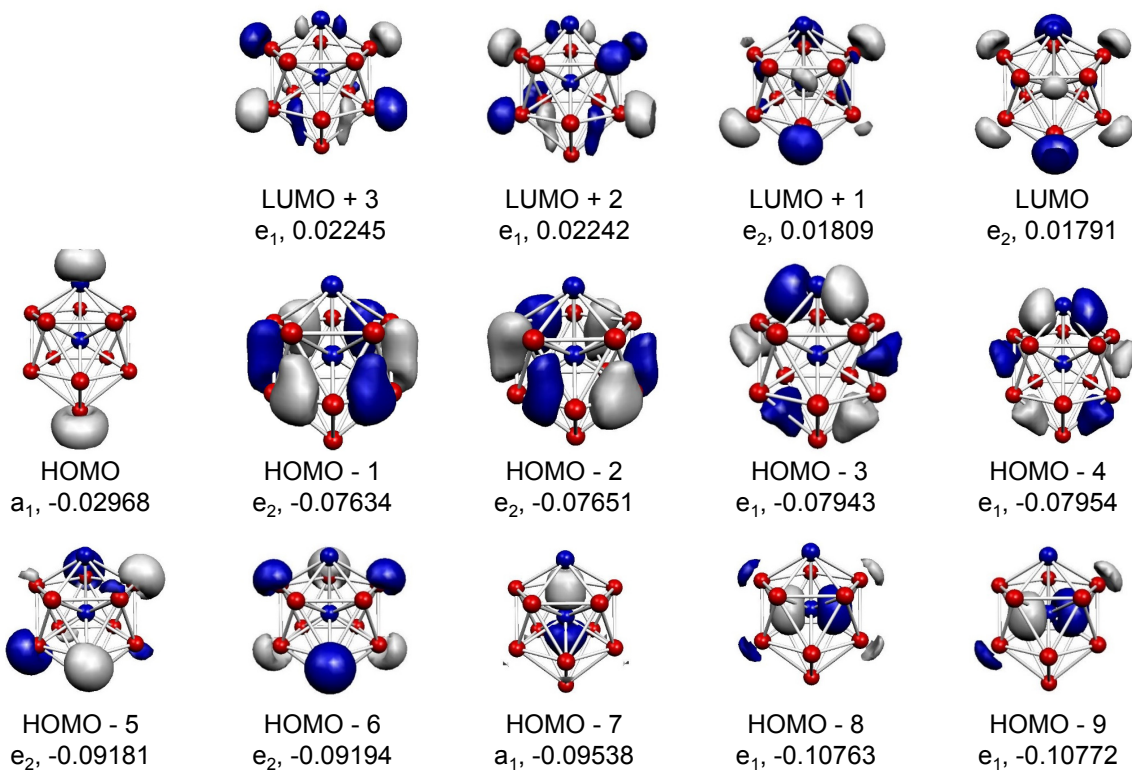


Figure S9. Occupied and virtual frontier orbitals from HOMO – 9 to LUMO + 4 for $\text{Al}_{11}\text{Si}_2^-$.

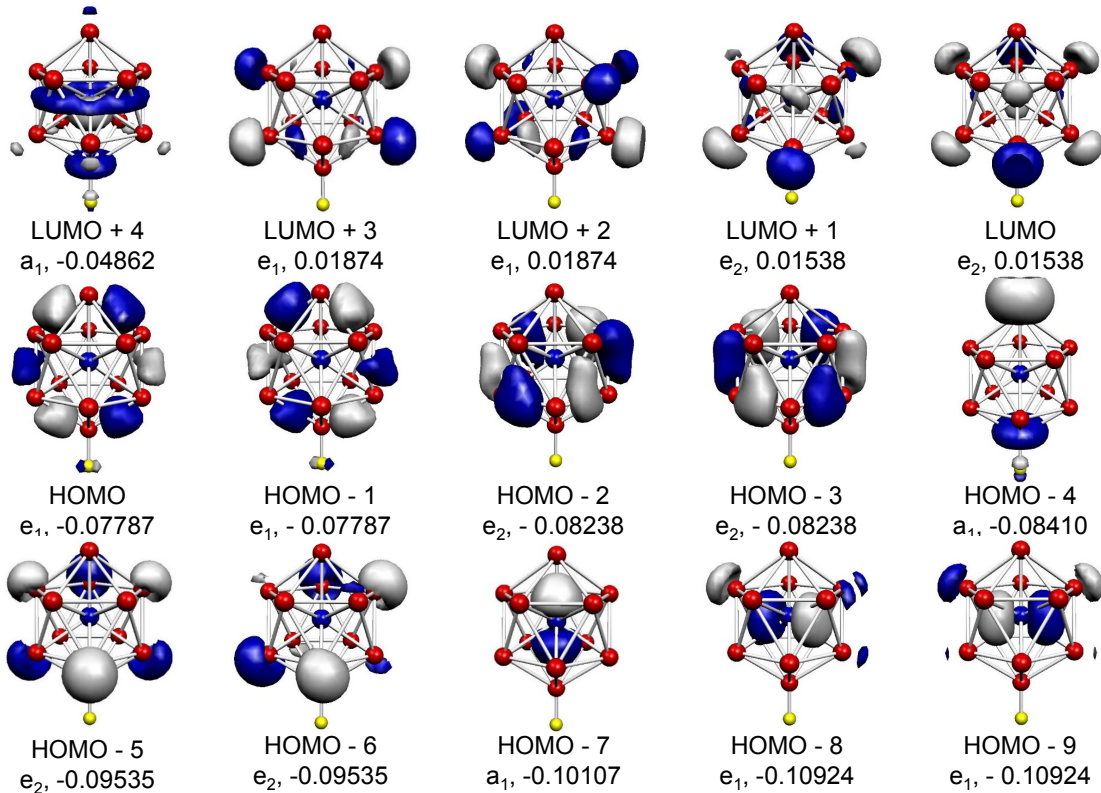


Figure S10. Occupied and virtual frontier orbitals from HOMO – 9 to LUMO + 4 for $\text{Al}_{12}\text{SiF}^-$.

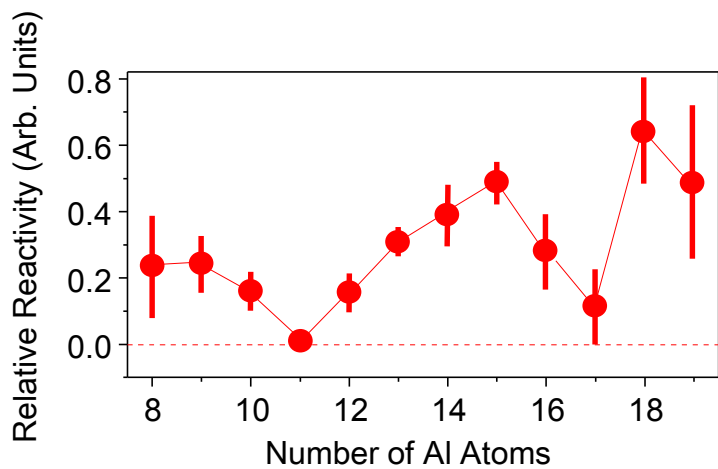


Figure S11. The relative reactivity for the cationic Al_nSi_2^+ clusters at $n = 8\text{--}19$ against O_2 molecules. Local maxima are observed at $n = 11$ and 17 . Both $\text{Al}_{11}\text{Si}_2^+$ and $\text{Al}_{17}\text{Si}_2^+$ satisfy the SAO closings of 2P ($40\text{ }e$) and 1G ($58\text{ }e$), respectively, and the low reactivities are explicable of electronic stability.

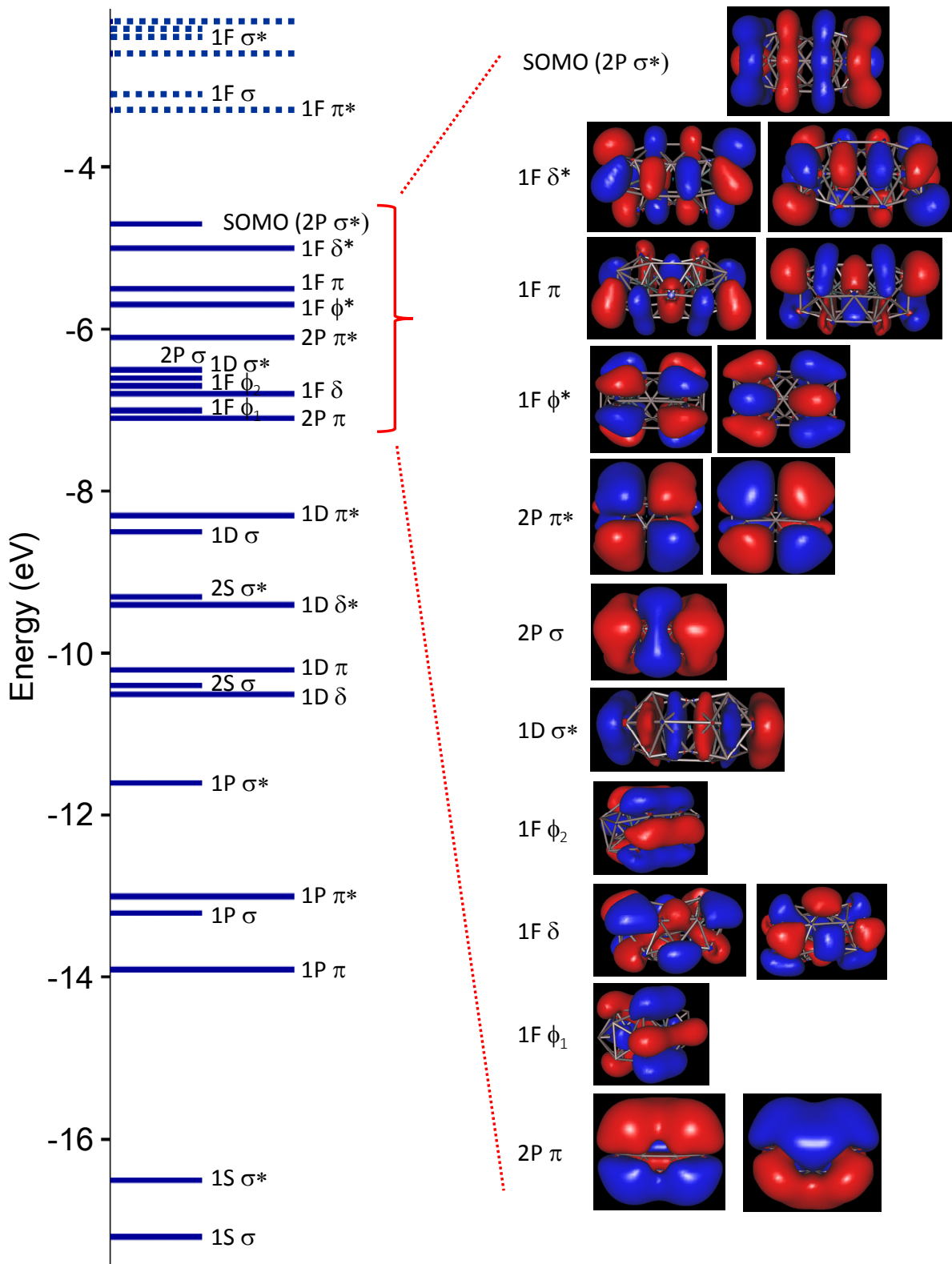


Figure S12. Calculated energy diagram and orbital shapes of LCSAO-MOs for *bi*-icosahedral $\text{Al}_{21}\text{Si}_2$. Solid lines show filled or half-filled states, whereas dotted lines do unoccupied states.

